

Supplementary Information

**Regulating Emissions of a *o*-Carborane-Based Molecule through
Molecular Vibrations Coupled with Molecular Orientations in Solid
States**

Junfeng Li, Shunan Shi, Yuhang Deng, Jiamian Ma, Wei Wu, Yu Chen, Yu Yan, and Wen-Yong Lai*

State Key Laboratory of Organic Electronics and Information Displays (SKLOEID), Institute of
Advanced Materials (IAM), School of Chemistry and Life Sciences, Nanjing University of Posts &
Telecommunications, 9 Wenyuan Road, Nanjing 210023, China

*E-mail: iamwylai@njupt.edu.cn

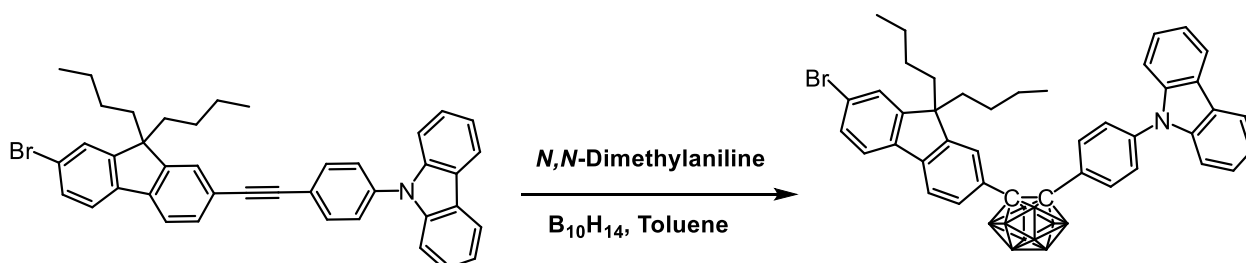
1. Instruments and materials

NMR spectra were recorded on a Bruker Ultra Shield Plus 400 MHz instruments with CDCl_3 as the solvent and tetramethylsilane (TMS) as the internal standard. UV-Vis spectra were obtained from a Perkin-Elmer Lambda 25 spectrometer. Fluorescent spectra were obtained with a 48000 DSCF spectrometer. Differential scanning calorimetry (DSC) profiles were measured on Netzsch DSC 200 F3. Thermo-gravimetric analysis (TGA) was performed on Shimadzu DTG-60A equipment. Time-resolved fluorescence decays were obtained from HORIBA JOBIN YVON Tem Pro-01 lifetime fluorescence spectroscopy. Absolute fluorescence/phosphorescence quantum yield was taken on Edinburgh Instruments' FLS980 fluorescence spectrophotometer attached with an integrating sphere. Raman spectroscopy was conducted on Horiba Labram Odyssey equipment. Single-crystal X-ray diffraction data collection and structure determination of *o*-1 was performed with an Xcalibur Onyx Nova four-circle diffractometer with a CCD system utilizing graphite-monochromatic $\text{Cu K}\alpha$ radiation ($\lambda = 1.54184 \text{ \AA}$). The empirical absorption correction was performed using the Crystal Clear program. The structure was solved using a direct method, and refined by full-matrix least-squares on F^2 employed in the program SHELXL-2016/6 program package. We employed the PLATON software/SQUEEZE subroutine to calculate the diffraction contribution of the solvent molecules and to generate a group of solvent-free diffraction intensities. The resulting new HKL file was used to further refine the structure. The crystallographic data and structure refinement parameters are summarized in Table S1, which contains the supplementary crystallographic data for this paper. *o*-1: CCDC number in 150 K, 193 K and 298 K was 2184818, 2270932 and 2184820, respectively. These data can be obtained free of charge from The Cambridge Crystallographic Data Centre.

Toluene and THF were purified by distillation from sodium in the presence of benzophenone.

Other chemicals were analytical grades and used without further purification.

2. Synthetic procedures and characterization



Synthesis of *o-1*: A mixture of decaborane ($B_{10}H_{14}$) (321.79 mg, 2.63 mmol), *N,N*-dimethylaniline (468.18 mg, 3.86 mmol) and 9-(4-((7-bromo-9,9-dibutyl-9H-fluoren-2-yl)ethynyl)phenyl)-9H-carbazole (1.00 g, 1.61 mmol) in anhydrous toluene (60 mL) was degassed for 30 min with a flow of nitrogen, and then the reaction mixture was refluxed 12 h. After being cooled to room temperature, the mixture was quenched by addition of methanol (30 mL). The organic phase was separated and the aqueous layer was extracted with CH_2Cl_2 (3×60 mL). The organic phases were combined, washed with brine, dried over anhydrous Na_2SO_4 and concentrated in *vacuo*. Purification by column chromatography (gradient of petroleum ether (bp. 60-90°C)/ CH_2Cl_2 , 90/10 to 80/20, v/v) afforded the title product (656.53 mg) in 55% yield as a white solid. The white single crystal was obtained from CH_2Cl_2 /MeOH in 70% yield. 1H NMR (400 MHz, $CDCl_3$, δ /ppm): 7.98-7.96 (m, 2H), 7.55 (d, $J = 12$ Hz, 2H), 7.50 (s, 1H), 7.42-7.37 (m, 3H), 7.34-7.28 (m, 2H), 7.23 (d, $J = 8$ Hz, 2H), 7.15-7.09 (m, 4H), 7.02-7.00 (m, 2H), 1.91-1.76 (m, 4H), 0.93 (td, $J = 8$ Hz, 12 Hz, 4H), 0.50 (t, $J = 8$ Hz, 6H), 0.46-0.41 (m, 2H), 0.38-0.29 (m, 2H). ^{13}C NMR (101 MHz, $CDCl_3$, δ /ppm): 152.44, 149.55, 141.27, 138.91, 138.51, 137.22, 131.10, 129.30, 128.48, 128.43, 128.20, 125.30, 125.08, 125.01, 124.97,

122.59, 121.41, 120.72, 119.43, 119.34, 118.20, 108.35, 85.42, 83.56, 54.38, 38.55, 24.66, 21.66, 12.57. ^{11}B NMR (128 MHz, CDCl_3 , δ/ppm): -2.42, -10.52.

3. NMR spectra

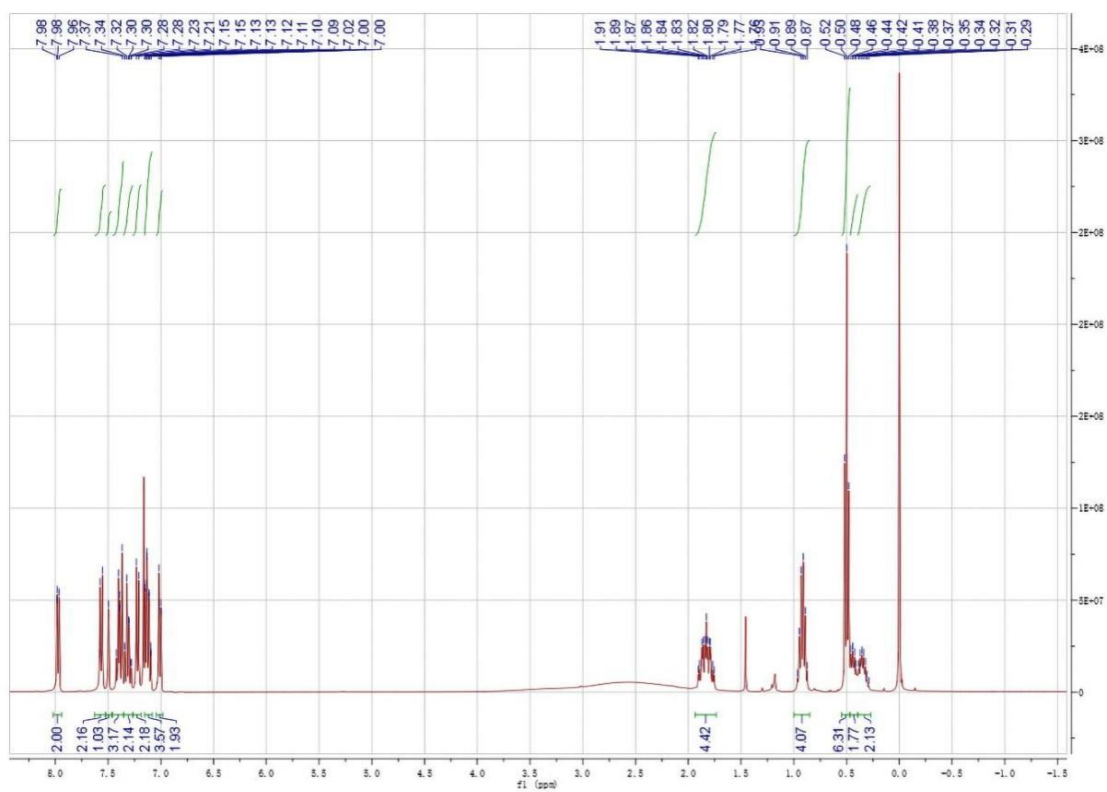


Figure S1. ^1H NMR spectra of *o*-I in CDCl_3 solution.

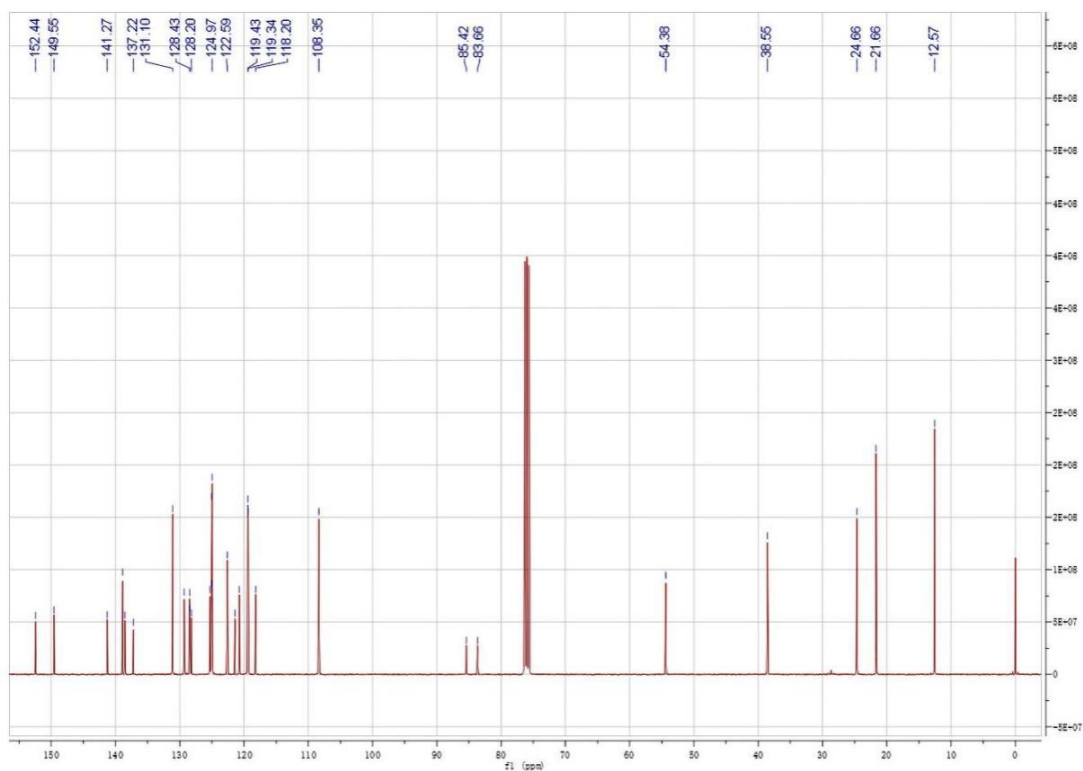


Figure S2. ^{13}C NMR spectra of *o-1* in CDCl_3 solution.

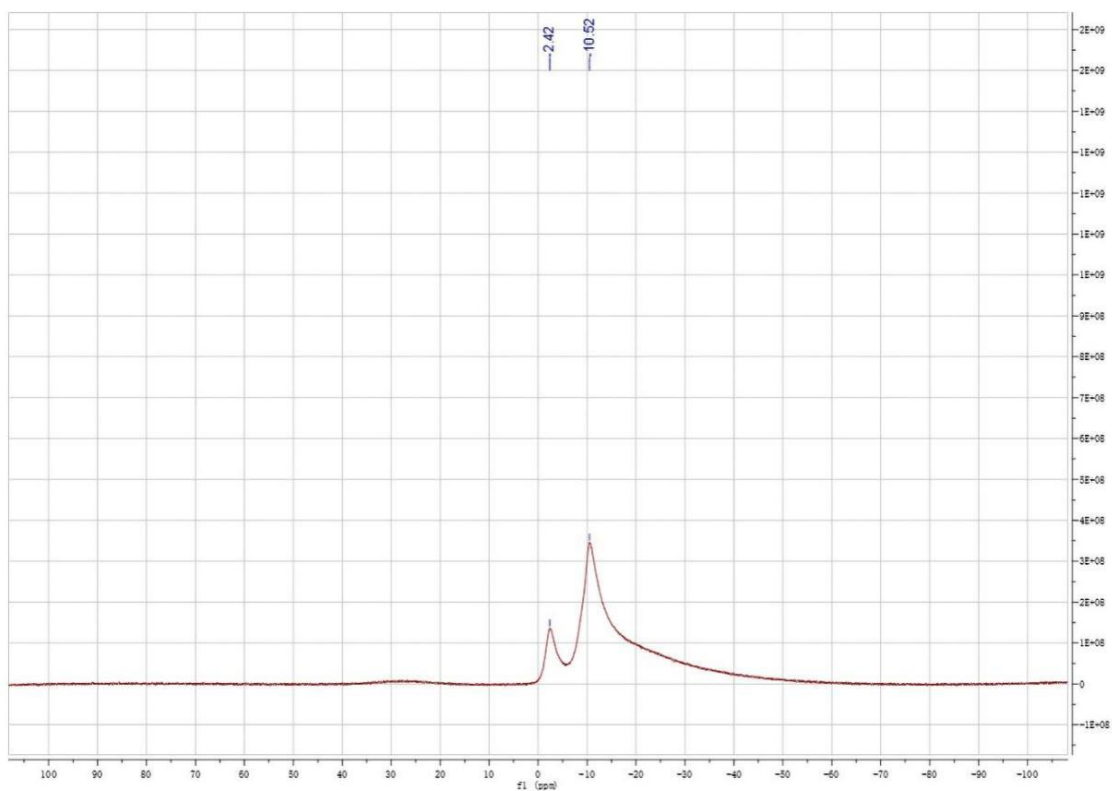


Figure S3. ^{11}B NMR spectra of *o-1* in CDCl_3 solution.

4. Thermo-gravimetric analysis

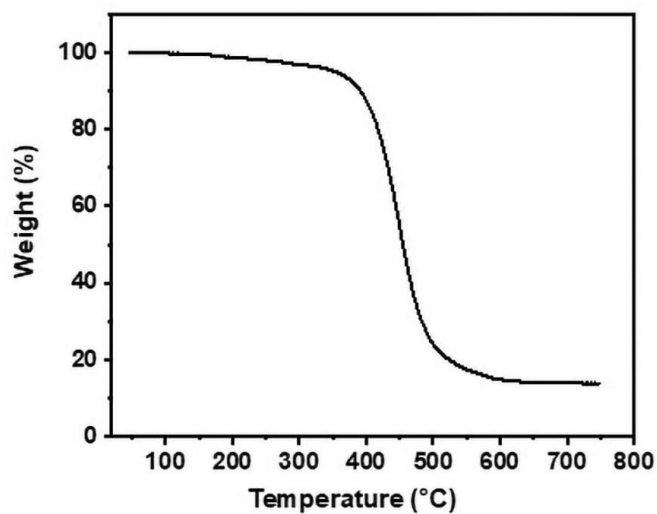


Figure S4. TGA profile of *o-I* in the the crystal states. The heating rate is 20°C/min. There was no decrease in the weight percent of the samples until decomposition. Its result indicated that both samples did not include solvent molecules in the crystals.

5. Aggregation-induced emissions

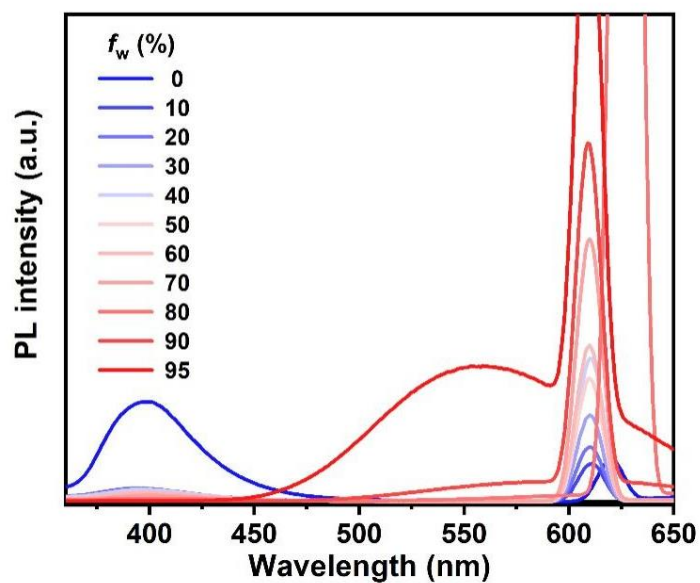


Figure S5. Emission spectra of *o-I* in THF, upon increasing the concentration water from 0% to 95% with concentration of 10 μM ($\lambda_{\text{ex}} = 310 \text{ nm}$).

6. Temperature-dependent UV-vis spectra in organic solvent

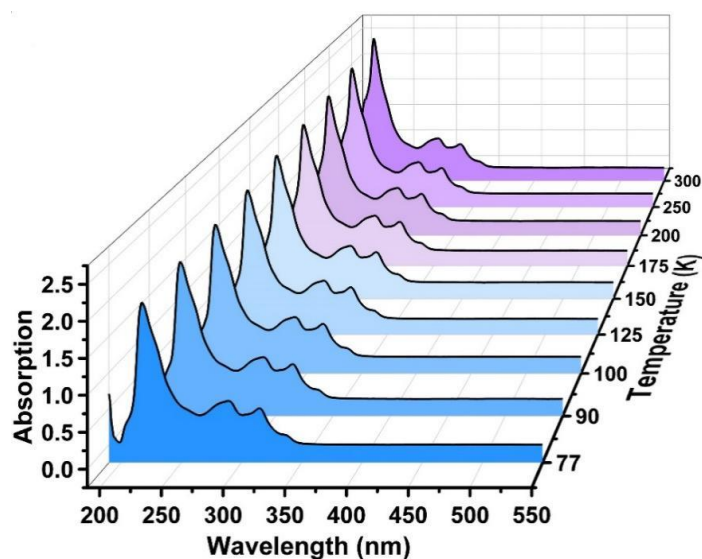


Figure S6. Temperature-dependent UV-vis spectra of *o-I* in the 1-chlorobutane solvent with concentration of 10 μM (Temperature: 77 K, 90 K, 100 K, 125 K, 150 K, 175 K, 200 K, 250 K, 300 K).

7. Temperature-dependent emission spectra in organic solvent

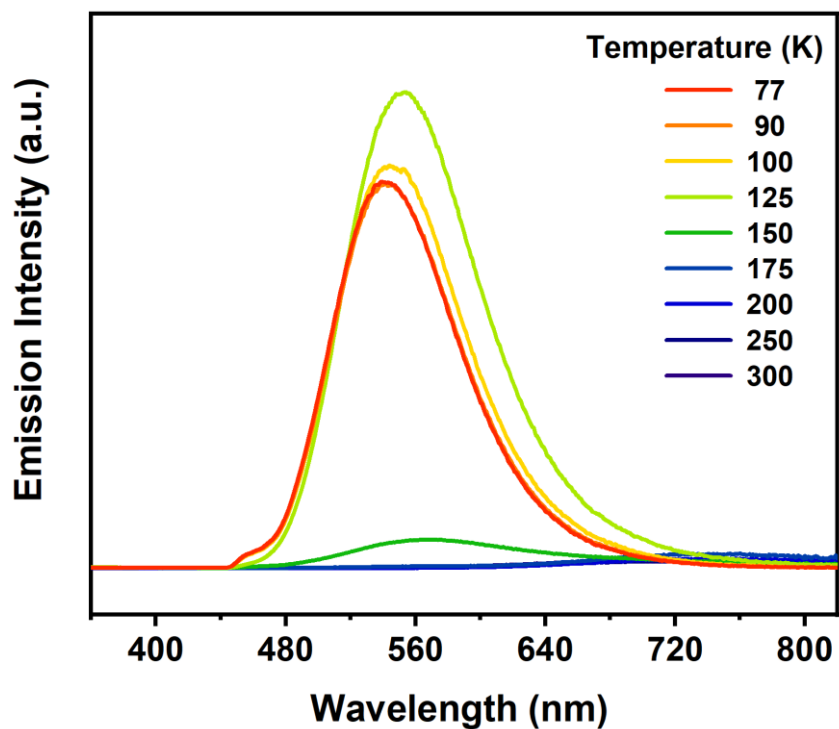


Figure S7. Temperature-dependent emission spectra of *o-I* in the 1-chlorobutane solvent with concentration of 100 μM (Temperature: 77 K, 90 K, 100 K, 125 K, 150 K, 175 K, 200 K, 250 K, 300 K).

8. Single crystal X-ray Diffraction

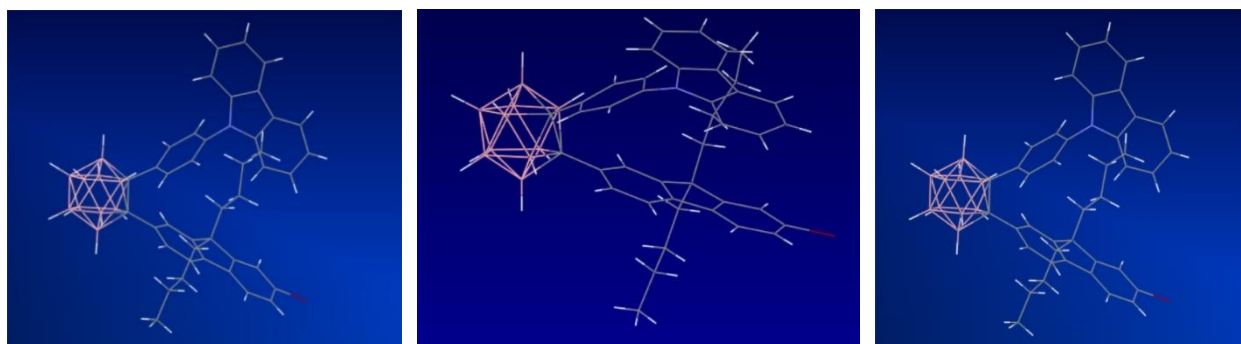


Figure S8. Crystal structure of *o-I* at 150 K (Left), 193 K (Middle) and 298 K (Right), respectively.

Table S1. Crystal Data and Structure Refinement for *o-1* at 150 K, 193 K and 298 K respectively.

Compound	<i>o-1</i> at 150K	<i>o-1</i> at 193 K	<i>o-1</i> at 298K
Empirical Formula	C ₄₁ H ₄₆ B ₁₀ BrN	C ₄₁ H ₄₆ B ₁₀ BrN	C ₄₁ H ₄₆ B ₁₀ BrN
Formula Weight	740.80	740.80	740.80
Temperature / K	150.00	193.00	298.00
Crystal System	triclinic	triclinic	triclinic
Space Group	P-1	P-1	P-1
a / Å	12.6933(4)	9.0254(4)	12.865(2)
b / Å	14.2351(5)	9.9212(4)	14.318(3)
c / Å	14.35585(5)	24.3778(12)	14.458(3)
α / °	111.2300(10)	86.455(3)	111.101(7)
β / °	109.4950(10)	85.978(3)	109.463(7)
γ / °	102.7280(10)	65.110(2)	103.101(7)
V / Å ³	2100.48(12)	1973.97(16)	2153.1(14)
Z	2	2	2
ρ _{calc} / g cm ⁻³	1.171	1.246	1.143
μ/mm ⁻¹	1.533	1.632	1.496
F (000)	768.0	768.0	768.00
Crystal size/mm ³	0.19 × 0.16 × 0.15	0.13 × 0.11 × 0.1	0.19 × 0.16 × 0.15
Radiation Cu K _α	λ = 1.54178	1.54178	λ = 1.54178
2θ range for data collection/°	7.228 to 136.764	7.274 to 136.802	7.2 to 137.136
Index ranges	-15 ≤ h ≤ 15, -17 ≤ k ≤ 17 -17 ≤ l ≤ 17	-10 ≤ h ≤ 10, -11 ≤ k ≤ 11, -29 ≤ l ≤ 29	-15 ≤ h ≤ 15, -17 ≤ k ≤ 17, -17 ≤ l ≤ 17
Reflections collected	62101	19282	60412
Independent reflections	7646 R _{int} = 0.0524 R _{sigma} = 0.0380	7167 R _{int} = 0.0532 R _{sigma} = 0.0614	7782 R _{int} = 0.0474 R _{sigma} = 0.0488
Data/restraints/parameters	7646/0/480	7167/0/480	7782/0/480
Goodness-of-fit on F ₂	1.060	1.066	1.074
Final R indexes [I ≥ 2σ (I)]	R ₁ = 0.0446 wR ₂ = 0.1200	R ₁ = 0.0441 wR ₂ = 0.1087	R ₁ = 0.0474 wR ₂ = 0.1340
Final R indexes [all data]	R ₁ = 0.0450 wR ₂ = 0.1203	R ₁ = 0.0577 wR ₂ = 0.1169	R ₁ = 0.0615 wR ₂ = 0.1426
Largest diff. peak/hole / e Å ⁻³	0.78-1.04	0.23/-0.58	0.34/-0.79

Bond Lengths for *o-1* at 298 K:

Atom	Atom	Length/Å	Atom	Atom	Length/Å
Br(1)	C(30)	1.896(2)	C(24)	C(27)	1.459(3)
N(1)	C(1)	1.400(3)	C(25)	C(26)	1.374(3)
N(1)	C(12)	1.386(3)	C(25)	C(33)	1.525(3)
N(1)	C(13)	1.431(3)	C(27)	C(28)	1.388(3)
C(1)	C(2)	1.384(4)	C(27)	C(32)	1.402(3)

C(1)	C(6)	1.414(3)	C(28)	C(29)	1.382(3)
C(2)	C(3)	1.391(4)	C(29)	C(30)	1.384(3)
C(3)	C(4)	1.388(5)	C(30)	C(31)	1.386(3)
C(4)	C(5)	1.368(5)	C(31)	C(32)	1.384(3)
C(5)	C(6)	1.386(3)	C(32)	C(33)	1.520(3)
C(6)	C(7)	1.436(4)	C(33)	C(34)	1.545(3)
C(7)	C(8)	1.400(4)	C(33)	C(38)	1.545(3)
C(7)	C(12)	1.412(3)	C(34)	C(35)	1.525(3)
C(8)	C(9)	1.361(5)	C(35)	C(36)	1.505(4)
C(9)	C(10)	1.403(5)	C(36)	C(37)	1.507(4)
C(10)	C(11)	1.368(4)	C(38)	C(39)	1.516(4)
C(11)	C(12)	1.388(4)	C(39)	C(40)	1.504(3)
C(13)	C(14)	1.380(3)	C(40)	C(41)	1.506(5)
C(13)	C(18)	1.375(4)	B(1)	B(2)	1.768(3)
C(14)	C(15)	1.381(3)	B(1)	B(6)	1.773(3)
C(15)	C(16)	1.393(3)	B(1)	B(7)	1.775(4)
C(16)	C(17)	1.388(3)	B(1)	B(8)	1.775(4)
C(16)	C(19)	1.502(3)	B(2)	B(3)	1.778(3)
C(17)	C(18)	1.388(3)	B(2)	B(7)	1.764(3)
C(19)	C(20)	1.731(2)	B(3)	B(4)	1.774(3)
C(19)	B(1)	1.713(3)	B(3)	B(7)	1.779(4)
C(19)	B(2)	1.728(3)	B(3)	B(9)	1.782(4)
C(19)	B(5)	1.721(3)	B(4)	B(5)	1.775(3)
C(19)	B(6)	1.706(3)	B(4)	B(9)	1.779(4)
C(20)	C(21)	1.493(3)	B(4)	B(10)	1.780(4)
C(20)	B(2)	1.727(3)	B(5)	B(6)	1.773(3)
C(20)	B(3)	1.707(3)	B(5)	B(10)	1.773(4)
C(20)	B(4)	1.714(3)	B(6)	B(8)	1.781(4)
C(20)	B(5)	1.724(3)	B(6)	B(10)	1.771(4)
C(21)	C(22)	1.399(3)	B(7)	B(8)	1.776(4)
C(21)	C(26)	1.401(3)	B(7)	B(9)	1.788(4)
C(22)	C(23)	1.382(3)	B(8)	B(9)	1.780(4)
C(23)	C(24)	1.387(3)	B(8)	B(10)	1.782(4)
C(24)	C(25)	1.399(3)	B(9)	B(10)	1.782(4)

Bond Lengths for o-1 at 193 K:

Atom	Atom	Length/Å	Atom	Atom	Length/Å
Br(01)	C(30)	1.898(2)	C(24)	C(27)	1.467(3)
N(1)	C(5)	1.399(3)	C(25)	C(26)	1.384(3)
N(1)	C(8)	1.388(3)	C(25)	C(33)	1.514(3)
N(1)	C(13)	1.428(2)	C(27)	C(28)	1.392(3)
C(1)	C(2)	1.377(4)	C(27)	C(32)	1.396(3)
C(1)	C(6)	1.398(3)	C(28)	C(29)	1.382(4)
C(2)	C(3)	1.391(4)	C(29)	C(30)	1.383(4)

C(3)	C(4)	1.383(3)	C(30)	C(31)	1.378(3)
C(4)	C(5)	1.385(3)	C(31)	C(32)	1.384(3)
C(5)	C(6)	1.409(3)	C(32)	C(33)	1.529(3)
C(6)	C(7)	1.438(4)	C(33)	C(34)	1.530(3)
C(7)	C(8)	1.414(3)	C(33)	C(38)	1.557(3)
C(7)	C(9)	1.394(3)	C(34)	C(35)	1.528(4)
C(8)	C(12)	1.392(4)	C(35)	C(36)	1.510(4)
C(9)	C(10)	1.373(4)	C(36)	C(37)	1.523(5)
C(10)	C(11)	1.399(4)	C(38)	C(39)	1.512(4)
C(11)	C(12)	1.377(4)	C(39)	C(40)	1.518(4)
C(13)	C(14)	1.384(3)	C(40)	C(41)	1.511(5)
C(13)	C(18)	1.389(3)	B(1)	B(2)	1.779(4)
C(14)	C(15)	1.388(3)	B(1)	B(3)	1.783(3)
C(15)	C(16)	1.395(3)	B(1)	B(8)	1.788(4)
C(16)	C(17)	1.385(3)	B(1)	B(9)	1.773(4)
C(16)	C(19)	1.508(3)	B(2)	B(3)	1.790(4)
C(17)	C(18)	1.386(3)	B(2)	B(4)	1.781(3)
C(19)	C(20)	1.716(3)	B(2)	B(10)	1.774(4)
C(19)	B(1)	1.705(3)	B(3)	B(4)	1.785(4)
C(19)	B(2)	1.710(3)	B(3)	B(5)	1.780(4)
C(19)	B(9)	1.737(3)	B(3)	B(8)	1.786(4)
C(19)	B(10)	1.725(3)	B(4)	B(5)	1.781(4)
C(20)	C(21)	1.501(3)	B(4)	B(6)	1.780(4)
C(20)	B(6)	1.707(3)	B(4)	B(10)	1.762(3)
C(20)	B(7)	1.713(3)	B(5)	B(6)	1.767(4)
C(20)	B(9)	1.726(3)	B(5)	B(7)	1.775(4)
C(20)	B(10)	1.739(3)	B(5)	B(8)	1.777(4)
C(21)	C(22)	1.393(3)	B(6)	B(7)	1.771(4)
C(21)	C(26)	1.401(3)	B(6)	B(10)	1.778(3)
C(22)	C(23)	1.388(3)	B(7)	B(8)	1.773(4)
C(23)	C(24)	1.385(3)	B(7)	B(9)	1.775(3)
C(24)	C(25)	1.397(3)	B(8)	B(9)	1.761(3)

Bond Lengths for o-1 at 150 K:

Atom	Atom	Length/Å	Atom	Atom	Length/Å
Br(1)	C(32)	1.900(2)	C(24)	C(29)	1.464(3)
N(1)	C(1)	1.399(3)	C(25)	C(26)	1.379(3)
N(1)	C(12)	1.392(3)	C(25)	C(27)	1.522(3)
N(1)	C(13)	1.426(3)	C(27)	C(28)	1.524(3)
C(1)	C(2)	1.387(3)	C(27)	C(34)	1.548(3)
C(1)	C(6)	1.413(3)	C(27)	C(38)	1.549(3)
C(2)	C(3)	1.386(3)	C(28)	C(29)	1.400(3)
C(3)	C(4)	1.397(4)	C(28)	C(33)	1.385(3)
C(4)	C(5)	1.376(4)	C(29)	C(30)	1.396(3)

C(5)	C(6)	1.399(3)	C(30)	C(31)	1.386(3)
C(6)	C(7)	1.441(3)	C(31)	C(32)	1.390(3)
C(7)	C(8)	1.398(3)	C(32)	C(33)	1.393(3)
C(7)	C(12)	1.409(3)	C(34)	C(35)	1.525(3)
C(8)	C(9)	1.377(4)	C(35)	C(36)	1.523(3)
C(9)	C(10)	1.404(4)	C(36)	C(37)	1.517(3)
C(10)	C(11)	1.384(3)	C(38)	C(39)	1.526(3)
C(11)	C(12)	1.388(3)	C(39)	C(40)	1.513(3)
C(13)	C(14)	1.381(3)	C(40)	C(41)	1.524(3)
C(13)	C(18)	1.386(3)	B(1)	B(2)	1.784(3)
C(14)	C(15)	1.394(3)	B(1)	B(6)	1.773(3)
C(15)	C(16)	1.390(3)	B(1)	B(7)	1.772(3)
C(16)	C(17)	1.395(3)	B(2)	B(3)	1.773(3)
C(16)	C(19)	1.504(3)	B(2)	B(7)	1.777(3)
C(17)	C(18)	1.388(3)	B(2)	B(8)	1.785(3)
C(19)	C(20)	1.727(2)	B(3)	B(4)	1.774(3)
C(19)	B(1)	1.728(3)	B(3)	B(8)	1.780(3)
C(19)	B(2)	1.702(3)	B(3)	B(9)	1.784(3)
C(19)	B(3)	1.709(3)	B(4)	B(5)	1.782(3)
C(19)	B(4)	1.729(3)	B(4)	B(9)	1.767(3)
C(20)	C(21)	1.496(3)	B(5)	B(6)	1.776(3)
C(20)	B(1)	1.728(3)	B(5)	B(9)	1.781(3)
C(20)	B(4)	1.730(3)	B(5)	B(10)	1.777(3)
C(20)	B(5)	1.708(3)	B(6)	B(7)	1.781(3)
C(20)	B(6)	1.712(3)	B(6)	B(10)	1.778(3)
C(21)	C(22)	1.402(3)	B(7)	B(8)	1.783(3)
C(21)	C(26)	1.403(3)	B(7)	B(10)	1.784(3)
C(22)	C(23)	1.390(3)	B(8)	B(9)	1.786(3)
C(23)	C(24)	1.387(3)	B(8)	B(10)	1.780(3)
C(24)	C(25)	1.402(3)	B(9)	B(10)	1.789(3)

9. Differential Scanning Calorimetry (DSC)

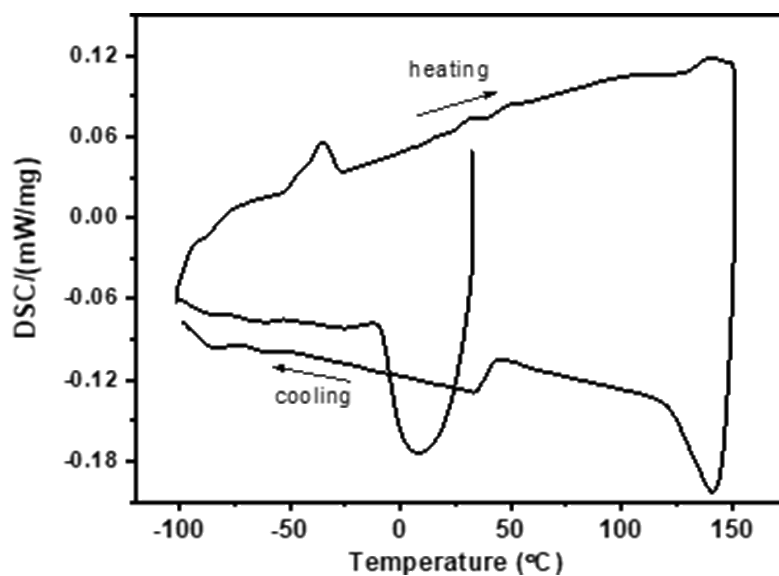


Figure S9. DSC profiles of *o-1* in the crystal states. Heating and cooling rates were 10°C /min, respectively. There were exo- or endo-thermic peaks in both crystalline samples.

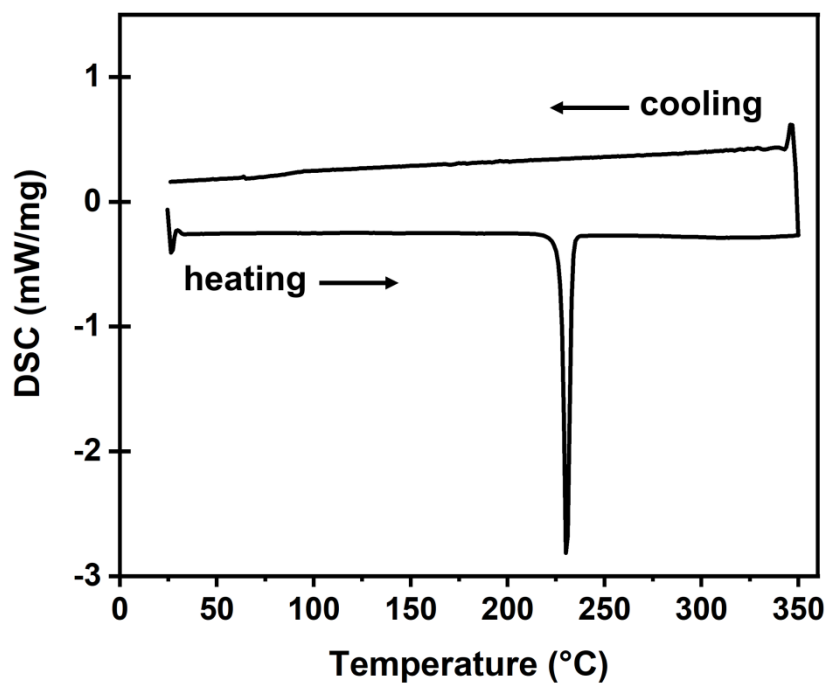


Figure S10. DSC profiles of *o-1* in the crystal states. Heating and cooling rates were 20°C /min.

There is endo-thermic peak in the crystal states.

10. UV-vis spectra in solid states

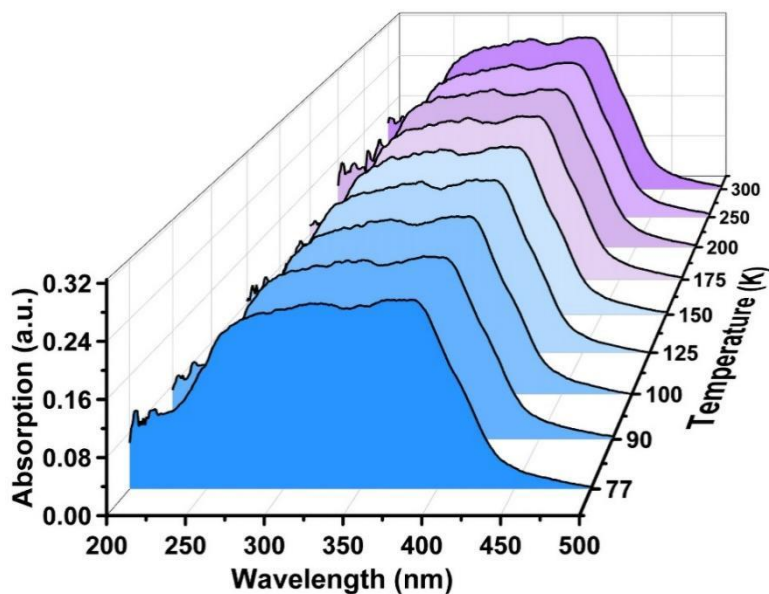


Figure S11. UV-Vis spectra of *o-1* in the solid states responding to various temperatures, including 77 K, 90 K, 100 K, 125 K, 150 K, 175 K, 200 K, 250 K, 300 K.

11. Analysis of fluorescence and phosphorescence

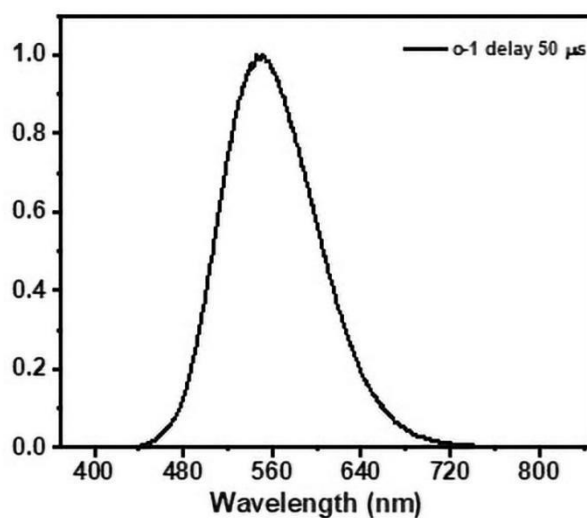


Figure S12. Delayed emissions of *o-1* in the crystal states with delayed times.

According to Maxwell-Boltzmann statistics, the equilibrium constant (K) of molecules in the CT and LE states at temperature is:

$$K = \frac{N_{CT}}{N_{LE}} = e^{-\Delta G/RT} \quad (1)$$

In which N is the population of each excited state, and N_{CT}/N_{LE} is equal to the concentration ratio [CT]/[LE] in the solution. The FL intensity (I) is directly proportional to the population of the excited states and the radiative decay rates:

$$I_i \propto N_i K_i \quad (2)$$

The CT/LE band ratio is written as eqn (3) using eqn (1) for the ratio of N_{CT}/N_{LE} :

$$\frac{I_{CT}}{I_{LE}} = \frac{N_{CT} k_{r,CT}}{N_{LE} k_{r,LE}} = \frac{k_{r,CT}}{k_{r,LE}} K = \frac{k_{r,CT}}{k_{r,LE}} e^{-\Delta G/RT} \quad (3)$$

where k_r is the radiative decay rate and ΔG is the energy difference between CT and LE states. Eqn (4) is linearized by taking the logarithm on both sides.

$$\ln \frac{I_{CT}}{I_{LE}} = \ln \frac{k_{r,CT}}{k_{r,LE}} + \frac{-\Delta G}{R} \frac{1}{T} \quad (4)$$

As the entropy difference between the LE and CT states is assumed to be very small ($\Delta S \approx 0$), ΔG is equal to ΔH and is thus not greatly affected by temperature; $k_{r,CT}$ and $k_{r,LE}$ are also constants in a certain temperature range. Thus, eqn (4) gives a linear dependence between the logarithm of the band ratio and $1/T$.

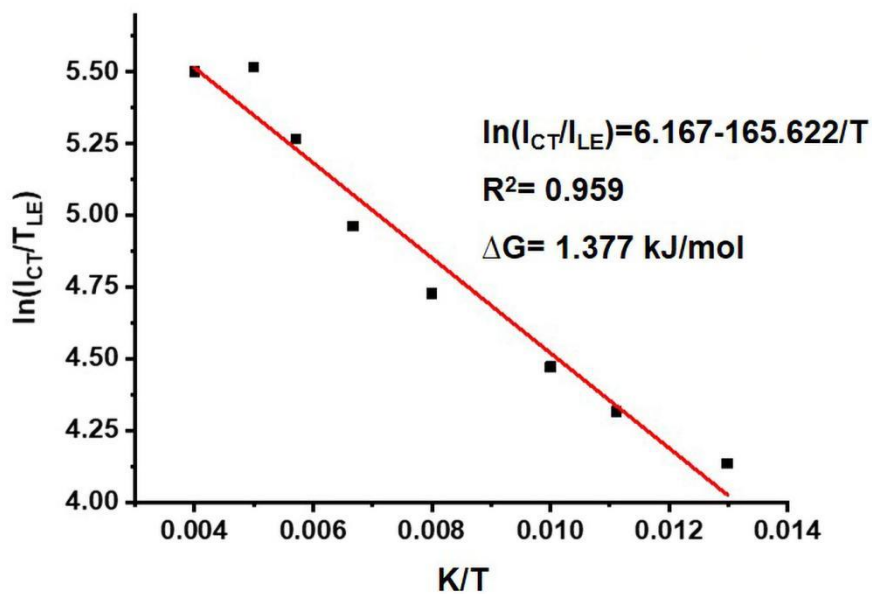


Figure S13. Stevens-Ban plot of *o-I* with corresponding ratio $\ln(I_{CT}/I_{LE})$ versus temperature, in which K is the equilibrium and T is the temperature.

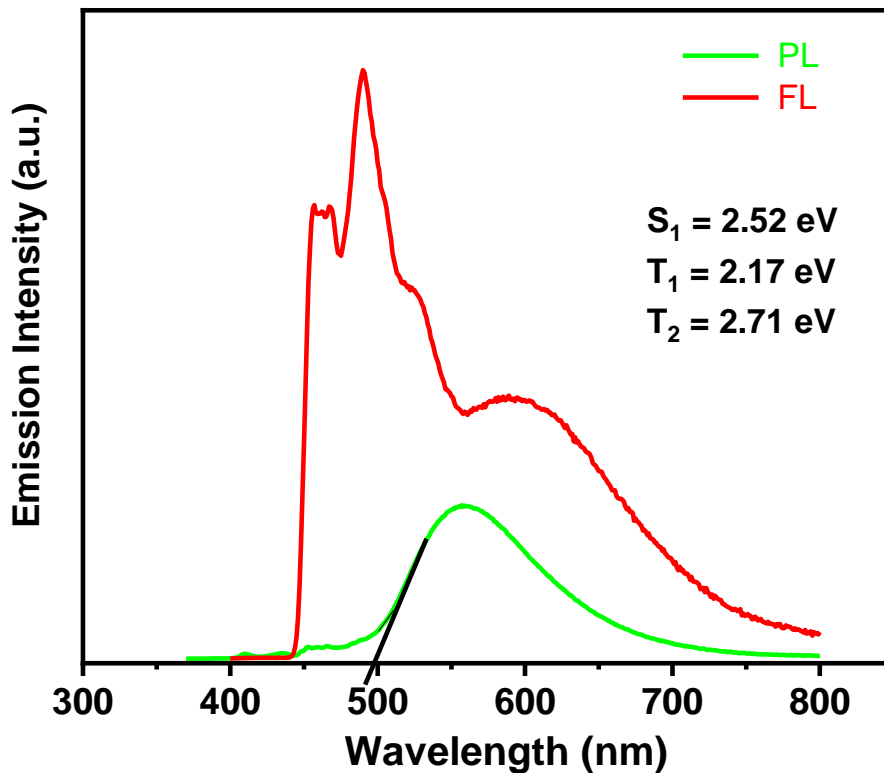


Figure S14. Prompt and delayed emission spectra *o-I* in the crystal states at 77 K, $\lambda_{exc} = 350 \text{ nm}$.

12. Theoretical calculations

We determined the vertical excitation energy of *o*-carborane-based molecule by optimizing its molecular structures extracted from various crystal structures using the Gaussian16 program package. Molecular structure optimization was performed at the PBE0/6-311G(d) level through Density Functional Theory (DFT) calculations.¹ Vertical excitation calculations were carried out at the TD-PBE0/def2-tzvp level. To enhance the accuracy of the excited state energy levels, we examined the potential energy surface of their triplet electronic states using Tamm-Dancoff Approximation density functional theory (TDA-DFT) with the PBE0/6-311G(d) functional. The transition density of these molecules was visualized and analyzed using Multiwfn 3.3.8 (dev) and VMD software.² The electron density functional theory (DFT) calculations have been carried out by the latest version of ORCA quantum chemistry software³ (Version 5.0.1). The Spin-Orbit Coupling (SOC) calculations were performed with PBE0 functional and the def2-tzvp basis set. SOC calculation was performed by spin-orbit mean-field (SOMF) method.⁴ The S₁ fluorescence emission of *o*-I corresponds to the LUMO to HOMO transition. Frontier molecular orbitals span the entire *o*-I molecule, with charge transfers from fluorene to carbazole, exhibiting distinct intramolecular charge transfer (ICT) properties. ³T₁ electron density was primarily located on the fluorene unit, designating it as the ³LE state. ³T₂ state, distributed mainly over the *o*-I molecule, demonstrated a clear intramolecular charge transfer from the *o*-carborane-based fluorene moiety to the carbazole unit, attributed to the ³CT state. The energy level gap between ³T₁ and ³T₂ was 0.763 eV, suggesting a rare probability of internal conversion. Notably, the ³CT₁ state exhibited a higher vertical energy state than the ³LE state.

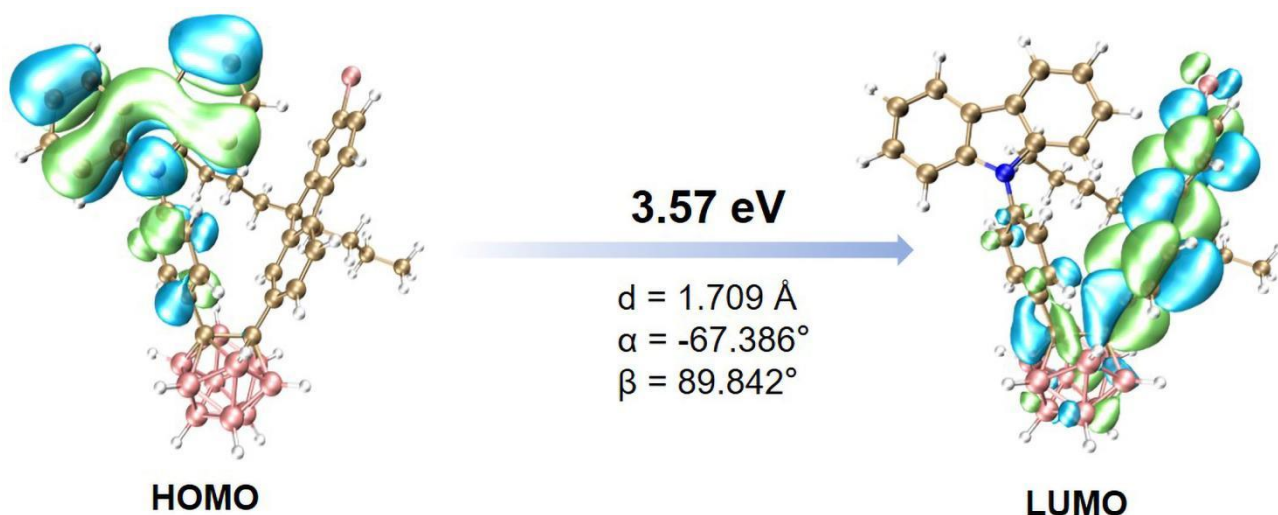


Figure S15. Frontier molecular orbitals and corresponding energy levels of *o-1* extracted from the crystal structure (*isovalue* = 0.02). The vertical energy of three molecules was calculated at the PBE0/def2-tzvp levels by TD-DFT calculations.

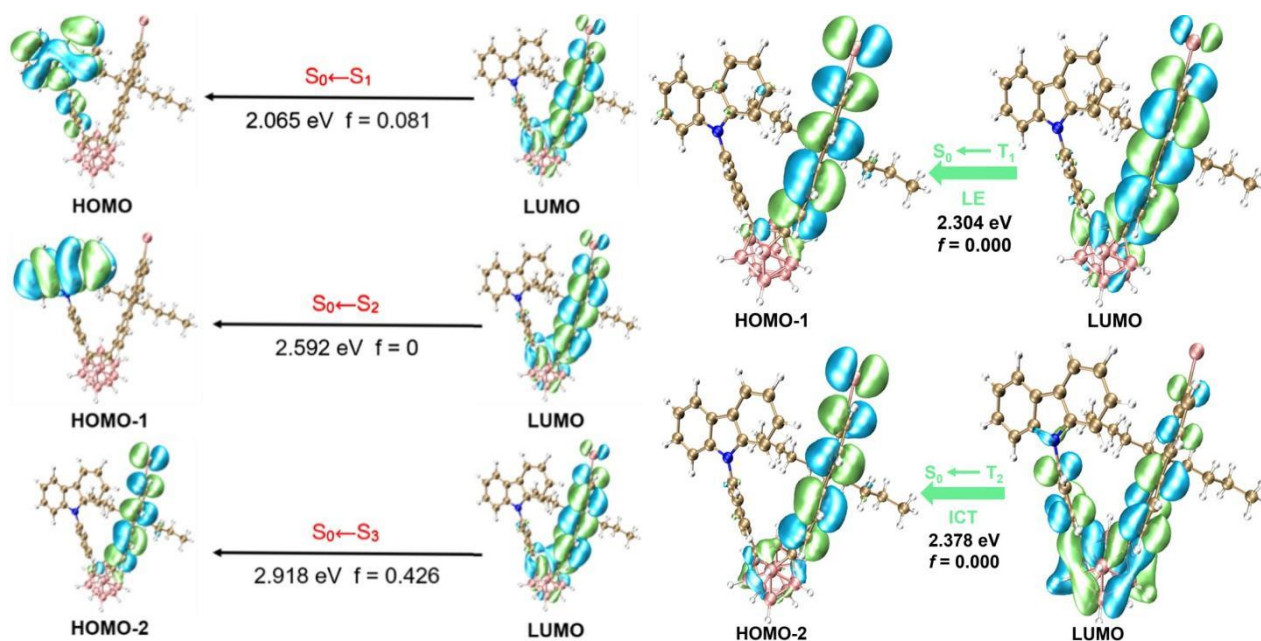


Figure S16. The singlet electron density distributions (*isovalue* = 0.02) of S_1 , S_2 , and S_3 for *o-1* were calculated at the TD-PBE0/6-311G(d) levels by TD-DFT calculation; the corresponding triplet electron density distributions (*isovalue* = 0.02) of T_1 , T_2 were calculated at TDA-PBE0/6-311G(d) levels by TD-DFT calculation.

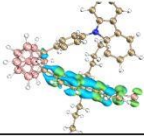
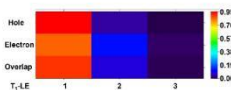
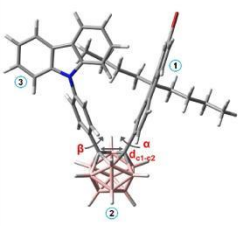

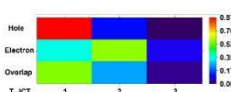

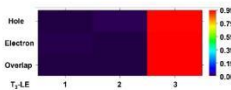
		Blue: Green:	Electron Hole	RMSD		
T_1	LE LE(82.45%) CT(17.55%)			0.107 Å		fragment1: 7-bromo-fluorenyl unit fragment2: o-carborane fragment3: 9-phenyl-carbazolyl unit 
T_2	ICT LE(37.28%) CT(62.72%)			0.257 Å		
T_3	LE LE(98.31%) CT(1.69%)			0.049 Å		

Figure S17. The hole (blue)–electron (green) triplet electron density distributions analysis (*isovalue* = 0.02) of T_1 , T_2 and T_3 for *o-1* were calculated at the optimized S_0 geometry in the gas at TDA-PBE0/6-311G(d) levels by TD-DFT calculations. Quantitative analysis of intramolecular charge transfer (CT) and local charge transfer (LE) in the excited states. Hot map of hole-electron analysis, and transferred electrons of paired fragments for *o-1*.

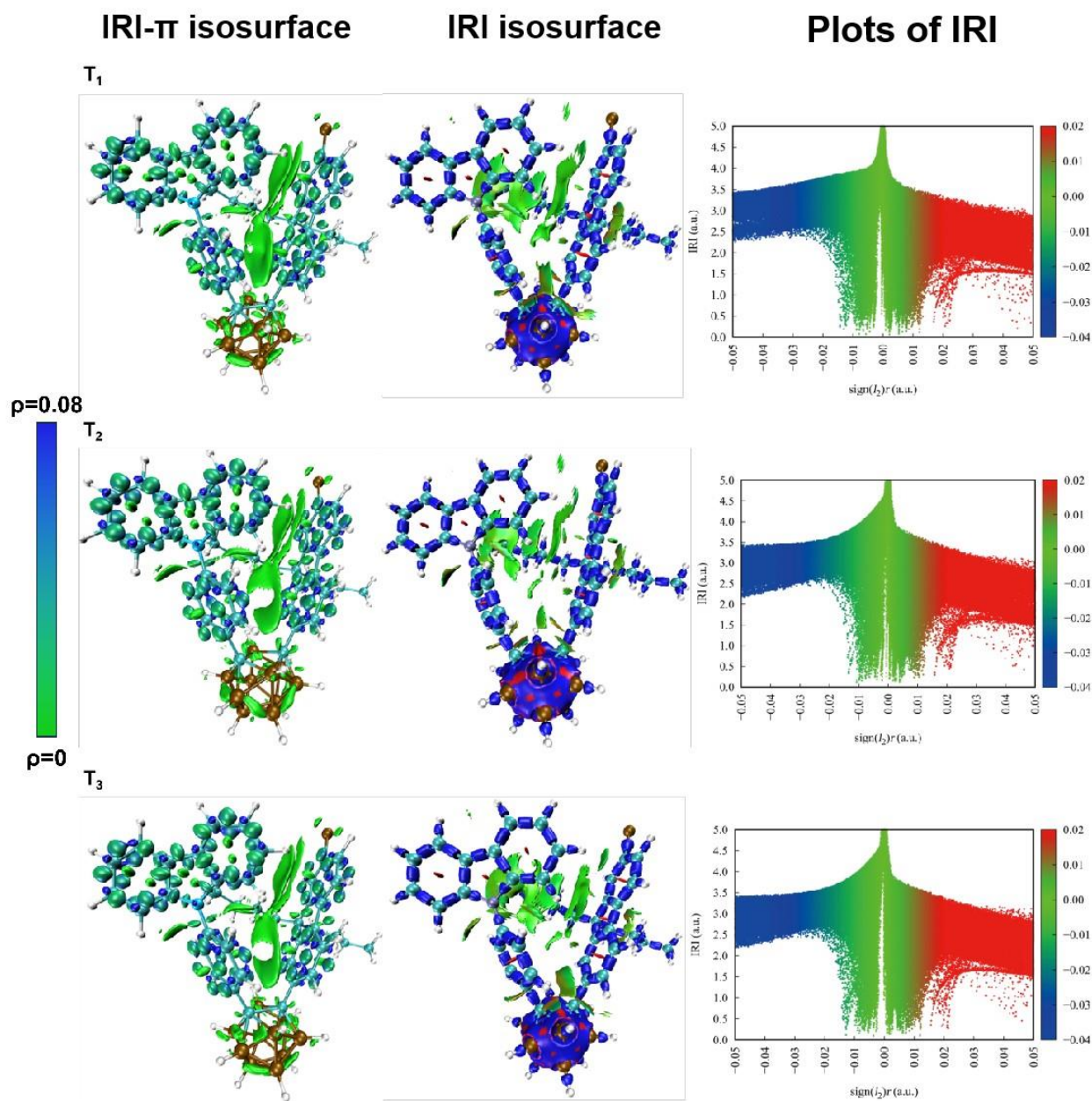


Figure S18. *IRI-π* isosurface of *o-1* showing the π interactions between intramolecular interactions.

IRI isosurfaces (*isovalue* = 0.6) of *o-1* in the T_1 , T_2 and T_3 states showing the weak intramolecular interactions. Blue and green isosurfaces represent the covalent interactions and weak interactions, respectively. Plots of *IRI* vs the electron density (ρ) of T_1 , T_2 and T_3 states multiplied by the sign of the second Hessian eigenvalue (λ_2).

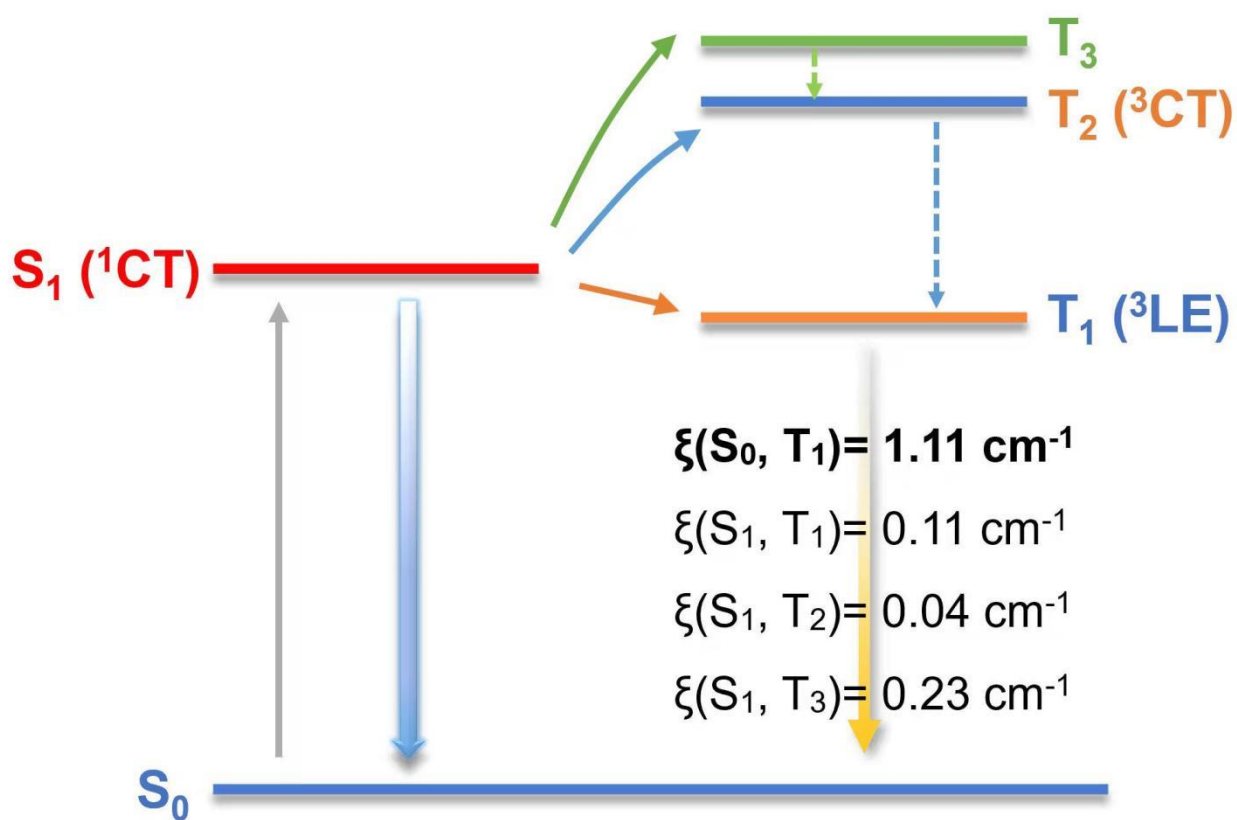


Figure S19. Vertical excitation energy levels of S_1 , T_1 , and T_2 for *o-I* were calculated at the optimized S_0 geometry in the gas phase at TD-DFT-PBE0/def2-tzvp level; spin-orbit coupling constants were calculated at the S_1 geometry.

13. Raman spectra in the solid states

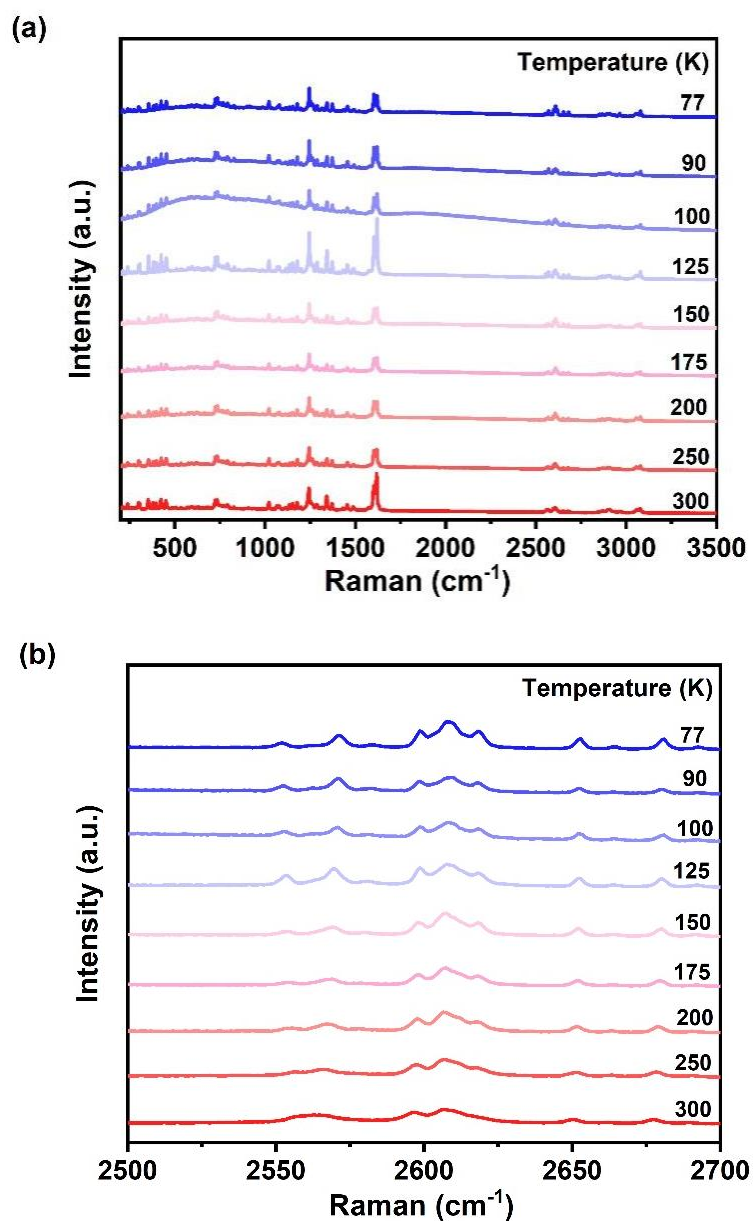


Figure S20. Raman spectra of *o*-I in the solid states responding to various temperatures, including 77 K, 90 K, 100 K, 125 K, 150 K, 175 K, 200 K, 250 K, 300 K.

References

1. M. J. Frisch, G. W. Trucks, H. B. Schlegel, G. E. Scuseria, M. A. Robb, J. R. Cheeseman, G. Scalmani, V. Barone, G. A. Petersson, H. Nakatsuji, X. Li, M. Caricato, A. V. Marenich, J. Bloino, B. G. Janesko, R. Gomperts, B. Mennucci, H. P. Hratchian, J. V. Ortiz, A. F. Izmaylov, J. L. Sonnenberg, Williams, F. Ding, F. Lipparini, F. Egidi, J. Goings, B. Peng, A. Petrone, T. Henderson, D. Ranasinghe, V. G. Zakrzewski, J. Gao, N. Rega, G. Zheng, W. Liang, M. Hada, M. Ehara, K. Toyota, R. Fukuda, J. Hasegawa, M. Ishida, T. Nakajima, Y. Honda, O. Kitao, H. Nakai, T. Vreven, K. Throssell, J. A. Montgomery Jr., J. E. Peralta, F. Ogliaro, M. J. Bearpark, J. J. Heyd, E. N. Brothers, K. N. Kudin, V. N. Staroverov, T. A. Keith, R. Kobayashi, J. Normand, K. Raghavachari, A. P. Rendell, J. C. Burant, S. S. Iyengar, J. Tomasi, M. Cossi, J. M. Millam, M. Klene, C. Adamo, R. Cammi, J. W. Ochterski, R. L. Martin, K. Morokuma, O. Farkas, J. B. Foresman, D. J. Fox, Gaussian, Inc., Wallingford, CT, Gaussian 16 Rev. C. 01.
2. T. Lu, F. Chen, *J. Comput. Chem.* **2011**, *33*, 580.
3. F. Neese, Software update: the ORCA program system, version 4.0. *Computational Molecular Science.* **2018**, *8*, e1327.
4. B. A. Heb, C. M. Marian, O. Gropen, *Chem. Phys. Lett.* **1996**, *251*, 365-371.